# Smart Polymeric Cathode Material with Intrinsic Overcharge Protection Based on a 2,5-Di-*tert*-butyl-1,4-dimethoxybenzene Core Structure

*Wei Weng, Zhengcheng Zhang,* Ali Abouimrane, Paul C. Redfern, Larry A. Curtiss, and Khalil Amine*

**Polymer-based electroactive materials have been studied and applied in energy storage systems as a valid replacement for transition metal oxides. As early as 1999, Hass et al. proposed an interesting concept on the possible incorporation of both charge storage and overcharge protection functionality into a single material. However, there are virtually no examples of polymeric materials that can not only store the charge, but also consume the overcharge current. Herein, a new material based on a cross-linked polymer (I) with 2,5-di-*tert*-butyl-1,4-dimethoxybenzene as the core structure is reported. The cyclic voltammogram of the synthesized polymer shows a single oxidation/reduction peak at 3.9–4.0 V. At 1C rate (56 mA/g), polymer I shows stable cycling up to 200 cycles with <10% capacity loss. The redox shuttle mechanism remarkably can be activated when cell voltage is elevated to 4.3 V and the overcharge plateau at 4.2 V (2nd plateau) is persistent for more than 100 hours. The overcharge protection was due to the release of a chemical redox shuttle species in the electrolyte during the initial charging process. Both DFT calculations and NMR analysis of the aromatic signals in the $^1$H-NMR spectrum of electrolytes from "overcharged" cells provide evidence for this hypothesis.**

## 1. Introduction

Lithium ion batteries have been used as a major power source for portable electronics. It has also been regarded as the most promising solution to electrify vehicles. The anticipated mass production of vehicle battery packs is limited by natural metal resources.[1,2] Recycling and disposal of used lithium-ion batteries are still challenging partially due to the presence of toxic heavy metals (Co and Ni are carcinogenic). Alternatively, organic based electro-active materials can be produced from sustainable resources with low cost and less environmental impact. With increased solubility in organic solvents, they have better processability and can be used for making flexible/paper batteries.[3]

Dr. W. Weng, Dr. Z. Zhang, Dr. A. Abouimrane, Dr. P. C. Redfern, Dr. L. A. Curtiss, Dr. K. Amine
Chemical Sciences and Engineering Division & Material Sciences Division
Argonne National Laboratory
9700 S. Cass Avenue, Lemont, IL 60439, USA
E-mail: zzhang@anl.gov

**DOI: 10.1002/adfm.201200458**

Just as researchers in the solar cell field have made vast progress in substituting silicon-based solar cells with polymer photovoltaic cells, the development of electro-active polymeric materials has also been the subject of intense research among the battery research community in the last few years. Electrochemically active polymers studied as electrode materials for energy storage include organic disulfide, conducting polymers (polythiophene, polyaniline etc.), radical polymers and polymers bearing anhydride, quinone or imide functionalities.[4–12]

We have pursued the synthesis of a new polymer cathode material based on our knowledge of redox shuttles (RS). The concept of redox shuttles is based on the working hypothesis that the RS molecule will lose an electron to form a cation radical ($RS^{\cdot+}$) at an intrinsic potential that depends on the nature of the compound. The oxidized form of the shuttle compound will diffuse to the negative electrode where it will gain an electron(s) and be reduced. The reversible redox couple RS/$RS^{\cdot+}$ thus shuttles the overcharge current that has been put into the battery between the electrodes at a defined voltage. The goal of this work was to incorporate this redox shuttle property into a polymer electrode with little voltage hysteresis between charge and discharge. In such polymers, active RS core structures are inter-connected with non-conjugated backbones so that the redox centers are isolated and independent from each other (**Figure 1**). Organic and organometallic based redox active molecules such as ferrocene,[8,9] anthraquinone,[11] etc. have been investigated as redox cores in polymeric materials for rechargeable batteries. A similar concept has been proposed by Hass et al.[13] in 1999, when they designed and synthesized poly(5-amino-1,4-naphthoquinone) (PNAQ). They envisioned that the quinone subunit could be lithiated and delithiated reversibly during charge and discharge process. The bystanding polyaniline backbone was anticipated to provide overcharge protection at higher potential. However, direct experimental evidences for this concept are lacking.

2,5-Di-*tert*-buyl-1,4-dimethoxybenzene (DDB) was reported as a promising shuttle candidate with an oxidation potential at 3.96 V *vs* $Li^+$/Li and good stability to survive more than 200

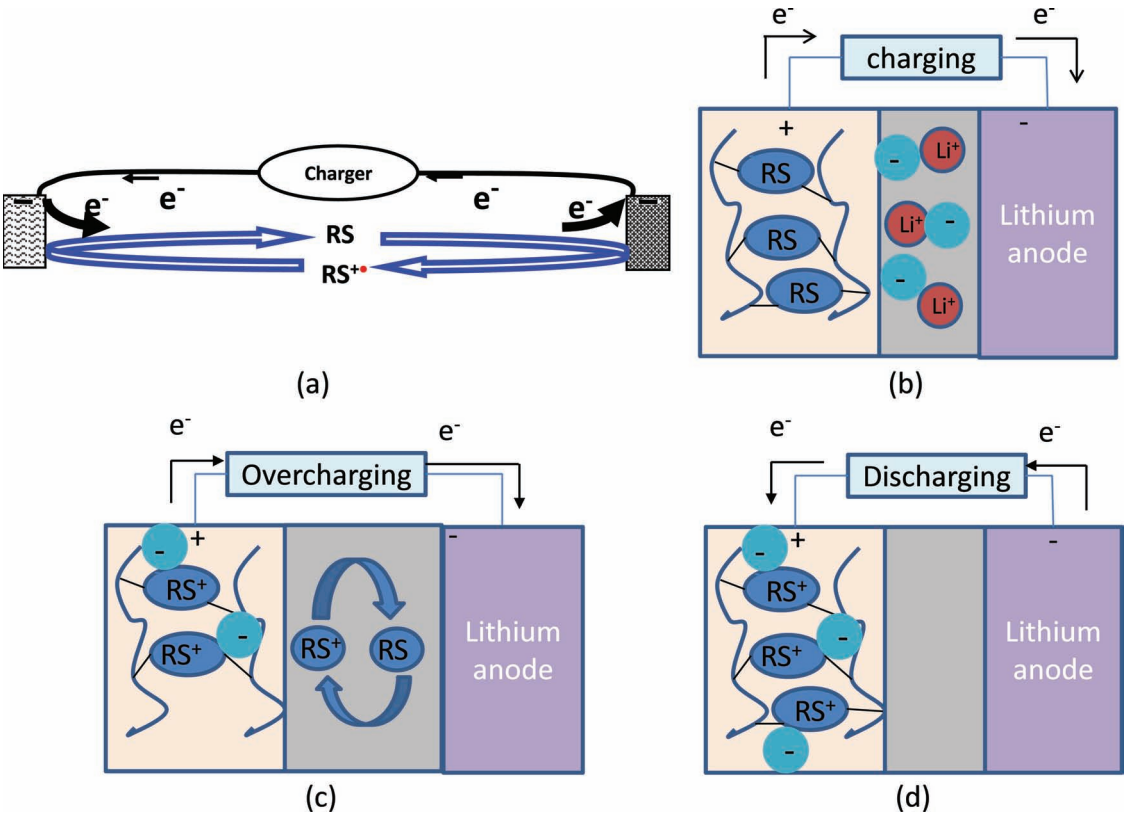


**Figure 1.** Proposed smart polymeric cathode material based on a RS core structure with intrinsic overcharge protection. (a) Shuttle mechanism of a redox shuttle molecule. (b) Charging of the polymer cathode/Li cell. (c) Overcharging of the polymer cathode/Li cell (voltage triggered overcharge protection). (d) Discharging of the polymer cathode/Li cell.

overcharge cycles.[14–16] From our past studies,[17,18] we have demonstrated that a few DDB-like compounds with reversible redox potentials in the range of 4.0–4.8 V can be used as redox shuttles to protect the positive electrode materials from overcharge damage (**Figure 2**).

In this study, we prepared a new polymer with a DDB core structure as the redox-active center cross-linked into a polymer matrix. This material can be charged and discharged under normal conditions (removal of 1e/RS unit). However, when the material is 100% overcharged (removal of 2e/RS unit), the RS-containing species are released from the polymer acting as an electron shuttle to provide overcharge protection for the polymer electrode (Figure 1). To the best of our knowledge, this is the first credible example of organic polymer cathode material with self-promoted overcharge protection function.

## 2. Results and Discussion

### 2.1. Synthesis and Characterization

Recently, Nesvadba reported the synthesis of a linear polymer from DDB based methacrylate monomer.[19] Unfortunately, this material is not suitable for making a polymer electrode due to its high solubility in conventional carbonate electrolytes. A non-electroactive crosslinker (ethylene glycol dimethacrylate, abbreviated EGDMA) has to be introduced in the polymerization step to decrease its solubility. Our approach is to use a self cross-linkable monomer to overcome this solubility problem. The synthesis strategy is shown in **Figure 3**. The monomer **II** can be obtained in moderate yield from two-step reaction. In the first step, 2,5-di-*tert*-butylhydroquinone was converted into the corresponding phenyl ether **III** by reaction with 3-bromo-1-propanol using $Cs_2CO_3$

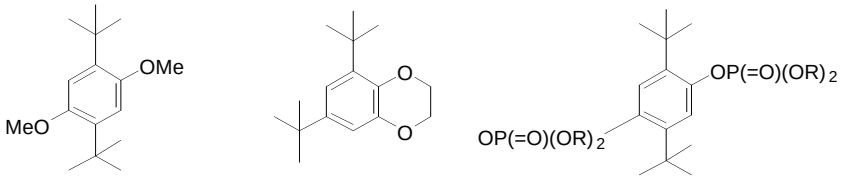


**DDB** 3.92 vs Li/Li+ **DBBD2** 4.17 vs Li/Li+ **TEDBPDP** (R=Et) 4.8 vs Li/Li+

**Figure 2.** Chemical structure and redox potential of some selected redox shuttles.

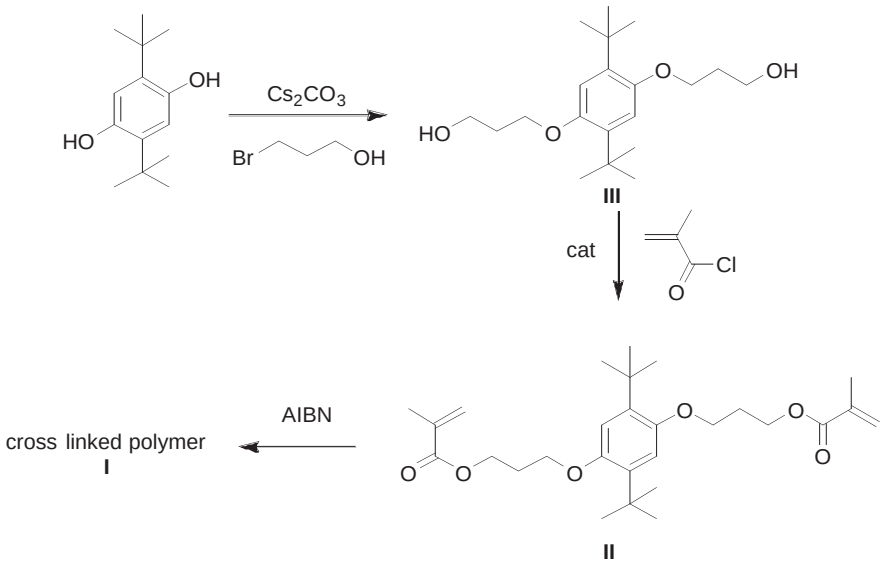


**Figure 3.** Synthesis of **II**, **III** and cross-linked polymer **I.**

as the base. The second step involves the simple esterification reaction of the hydroxyl group in **III** with methacryloyl chloride in the presence of triethylamine. In the $^1$H NMR spectrum (**Figure 4**), the terminal acrylate olefin protons in monomer **II** resonate at 6.13 and 5.57 ppm, respectively. Also there are three downfield shifted methylene groups in **II** compared to **III** due to the greater electron withdrawing ability of acrylate in **II** than hydroxyl group in **III**. (Figure 4, a: from $\delta$ 4.1 to 4.3 ppm; b: from 3.92 to 4.08 ppm; c: from 2.09 to 2.21 ppm). As also evidenced in the $^{13}$C NMR spectrum, the characteristic NMR peaks for the acrylate are 136.2 and 136.1 ppm for olefin carbons and 167.3 ppm for the carbonyl group. The cross-linking polymerization of **II** was initiated with 2,2′-azobis(2-methylpropionitrile) (AIBN) in toluene solution. The synthesized polymer is insoluble in common organic solvents (i.e., dimethyl carbonate) unlike the polymer from the mono-acrylate monomer.[19] **Figure 5** shows the FT-IR spectra of the monomer **II** and its cross-linked polymer **I**. The characteristic peaks for C = C in **II** (C = C stretching: 1640 cm$^{-1}$, C = C out of plane stretching: 936 cm$^{-1}$ and 817 cm$^{-1}$) disappear upon polymerization.[20] In addition, the stretching vibrations of ester C = O of acrylate also shift from 1710 cm$^{-1}$ in the monomer to 1729 cm$^{-1}$ in the cross-linked polymer due to the removal of conjugation between C = O and C = C in acrylate during the polymerization.

## 2.2. Electrochemical Properties

### *2.2.1. Cyclic Voltammograms of I*

The synthesized polymer cathode was prepared by casting a slurry of active polymer **I** with super P carbon black as the conductive additive and PVDF as the binder on an aluminum foil current collector. A 2032 coin cell was configured with a negative electrode (Li foil), polyolefin separator (celgard 2325) and the polymer cathode **I**. **Figure 6** shows the cyclic voltammetry (CV) profiles for the polymer material with a scan rate of 0.05 mV/s. During the first cycle sweep, the CV curve shows a single oxidation peak centered at 4.02 V and reduction peak located at 3.92 V *vs.* Li/Li$^+$. In the second cycle, the oxidation peak slightly moved to a higher potential and the reduction peak moved to a lower potential. After the second cycle sweep, the shape of the CV curve does not change significantly, indicating a reversible redox reaction between the neutral form and radical cation form.

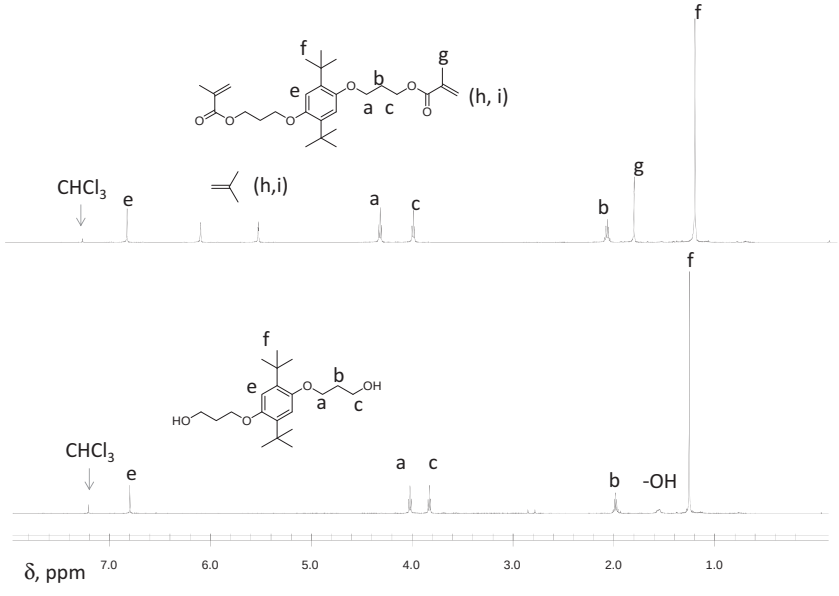


**Figure 4.** $^1$H NMR spectra of **II** and **III.**

### *2.2.2. Polymer I/Li Cell Cycling Property at Regular Charge Condition*

The charge-discharge voltage profiles (first two cycles) and cycling stability of the polymer material with a current density of 56 mA g$^{-1}$ with cutoff voltage of 4.1–3.0 V is shown in **Figure 7**. Well-defined charge and discharge plateaus with a small voltage gap are observed as shown in Figure 7a. The charge and discharge voltages are also quite consistent with the oxidation and reduction potentials determined by the CV experiment.

A galvanostatic cycling test at 1*C* rate reveals that the initial specific charge capacity of 61 mAh/g is obtained, slightly greater than the theoretical capacity calculated from the 1e process (56 mAh/g). The discharge capacity in the first cycle is 38 mAh/g, which corresponds to a coulombic efficiency of 63%. The relative high irreversible capacity loss

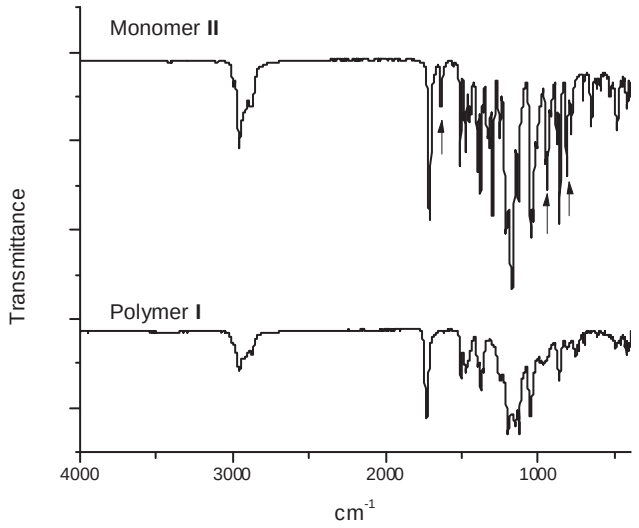


**Figure 5.** FT-IR spectra of monomer **II** and cross-linked polymer **I.**

observed is also in accordance with the previously reported DDB-co-EGDMA polymer.[19] The discharge capacity increased to 41 mAh/g in the second cycle with a coulombic efficiency of 87%. The cell maintained stable capacity up to 200 cycles, where the capacity retention is >90% of the capacity of the 2nd cycle. Polymer **I** shows better cycling stability than DDB-co-EGDMA, which delivers a similar capacity with 1.5% capacity fading per cycle for 90 cycles.[19]

### *2.2.3. Polymer I/Li Cell Cycling Property at Overcharge Condition*

This material displays an interesting phenomenon during overcharge. **Figure 8** shows the voltage profile from charging the polymer **I**/Li cell at 1*C* rate for 2 h (i.e. charging to 200% of its theoretical capacity, or 100% overcharge), and then discharging the cell to 3.0 V. As shown in Figure 8, the normal charge took place at 3.80–4.05 V. After the cell was fully charged, the voltage climbed up quickly to 4.2 V and maintains a plateau at this voltage, where the shuttle mechanism was activated. The second plateau at 4.2 V indicates that the overcharge current was consumed by the reversible oxidation/reduction of some species which is formed from the oxidation of the polymer cathode at high potential and dissolves in the electrolyte. This species diffuses between the positive and negative electrode. The amount of the dissolved redox shuttle is probably small because after the first overcharge, the discharge capacity of the cell is 34 mAh/g, which is more than 85% of the normal discharge capacity at 1*C* rate. As shown in **Figure 9**, the overcharge plateau is only slightly elevated and the cell voltage is still well controlled after more than 40 overcharge cycles with discharge capacity retention of 70% compared with the initial value.

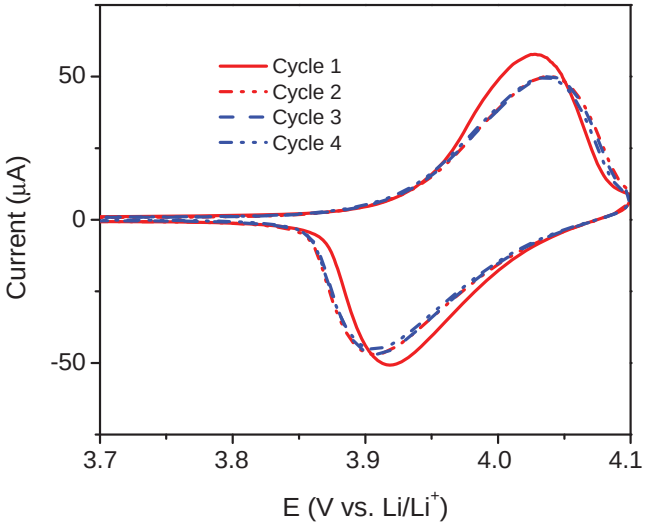


**Figure 6.** Cyclic voltammograms of cross-linked polymer **I** (scan rate: 0.05 mV/s).

Apparently, the shuttle species is generated from the polymer cathode. The cross-linked polymer was speculated to be broken down into either small chains or single molecules containing the RS core structure during the overcharge cycles. To probe the origin of the shuttle mechanism, the polymer **I**/Li cells were charged with a current density of 7 mA/g for 110 hours (limiting voltage 4.3 V), and then disassembled in a glove box. The electrolyte was recovered by rinsing the cell parts with dimethyl carbonate (DMC) solvent. After removal of the DMC, the remaining electrolyte residue was analyzed by NMR spectroscopy, as shown in **Figure 10**. The aromatic signals at 6.2–7.2 ppm and *tert*-butyl signal at 1.24 ppm confirm the presence of the DDB core-containing species generated and dissolved in the electrolyte during the polymer cathode charging process. The $^{1}$H NMR spectrum shows two pairs of doublets in the aromatic region, one pair centered at 7.05 and 6.76 ppm with a coupling constant of 8 Hz and the other pair centered at 6.35 and 6.23 ppm with a coupling constant of 4 Hz, which are consistent with typical *ortho* and *meta* proton coupling in the benzene ring. The presence of doublets indicates a lower symmetry in the redox shuttle mediator than the precursor **II** or **III** (only one singlet was observed). It is likely a chemical bond breaking process is involved in the formation of redox shuttle. The GC/MS was employed to analyze the electrolyte after cycling. Multiple elution peaks with molecular mass with a range from 190 to 429 were detected. We have not been able to conclusively identify the redox mediators based on NMR and GC data; there should be at least three benzene containing species which can act as redox shuttle candidates.

## 2.3. Computational Studies

### *2.3.1. Redox Shuttle Candidates and Their Oxidation Potentials*

Density functional theory (DFT) calculations were carried out to investigate the feasibility that the oxidized cross-linked polymeric cathode with the DDB core structure might release a DDB fragment that subsequently has an oxidation potential acting as a redox shuttle. In previous work we have used DFT calculations to theoretically determine the oxidation potential of

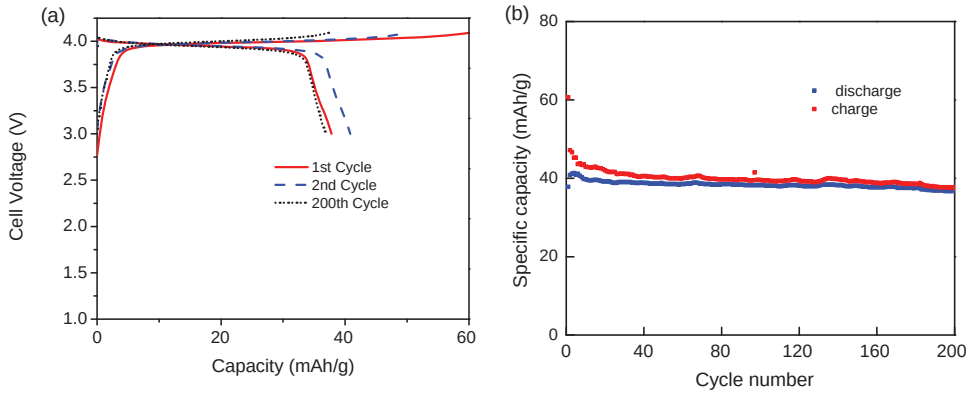


**Figure 7.** a) Charge-discharge voltage profiles. b) Galvanostatic cycling performance of polymer **I**/Li cell with 1*C* rate.

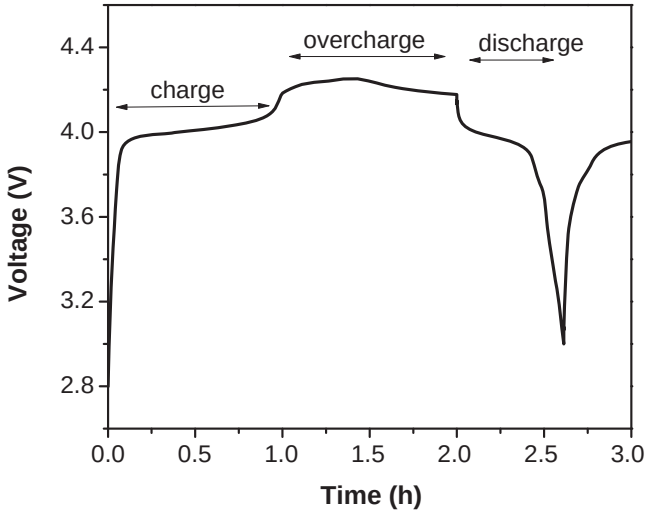


**Figure 8.** Typical voltage profile of the polymer **I**/Li cell at 100% overcharge condition (charge for 2 hours and then discharge to 3.0 V at 1*C* rate).

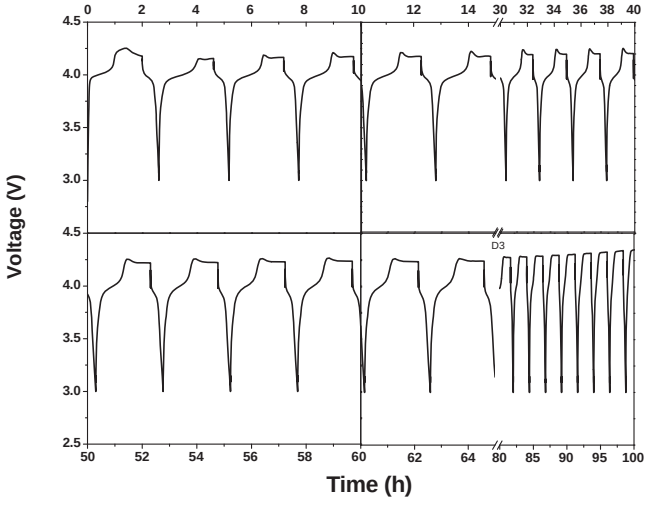


**Figure 9.** Voltage profile of the polymer **I**/Li cell with 100% overcharge for extended cycles (charge for 2 hours and then discharge to 3.0 V at 1*C* rate).

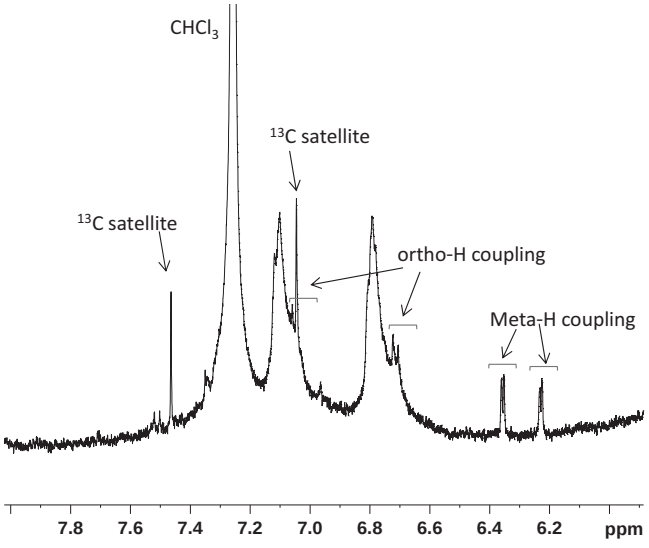


**Figure 10.** $^{1}$H NMR spectrum ($\delta$ 6 ~ 8) of the electrolyte residue extracted from the overcharged polymer **I**/Li cells.

other redox shuttles as well as their decomposition pathways.[18] Since there are many possible decomposition mechanisms for the polymer cathode with a DDB core structure upon oxidation, we first investigated the oxidation potentials of various possible products that could act as subsequent redox shuttles. A few possible decomposition products produced from combinations of C-O and/or C-C bond cleavage are illustrated in **Figure 11**. Some of the compounds have an oxidation potential close to 4.2 V vs $Li^{+}$/Li. For example, 2,5-di-*tert*-butyl-1-methoxybenzene could result from breaking an O bond to a C of the aromatic ring on one linker group (type b) and the C-C bond nearest to the aromatic ring on the other linker. The calculated oxidation potential of the 2,5-di-*tert*-butyl-1-methoxybenzene is 4.29 V compared to 3.82 V for the model for the parent DDB molecule with ether arms in the polymer matrix as shown in Figure 11. The calculated results compare favorably with the two oxidation peaks observed experimentally at 3.9 and 4.2 V (Figure 8). The higher oxidation potential for 2,5-di-*tert*-butyl-1-methoxybenzene is due to the removal of an electron donating OMe group

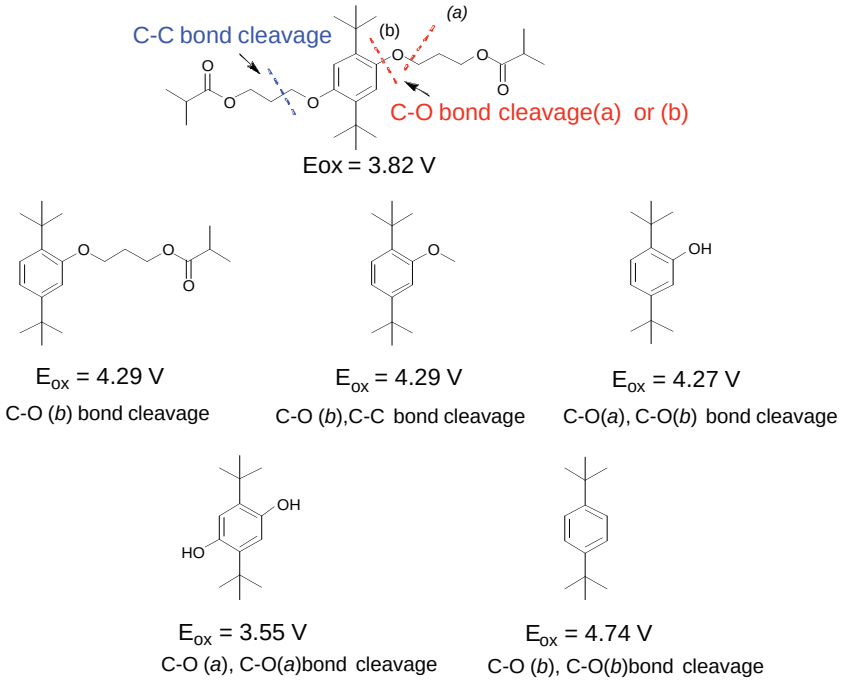


**Figure 11.** Possible redox shuttles resulting from the cross-linked polymeric material with their oxidation potentials.

from the benzene ring. This is also in line with previous experimental studies of other DDB based redox shuttles.[21,22] Another decomposition product could be 2,5-di-*tert*-butyl-phenol formed from breaking an O bond to a C of the aromatic ring on one linker group (type b) and the O-C bond nearest to the aromatic ring on the other linker (type a) with an oxidation potential of 4.27 V (Figure 11). Other possibilities that were considered are 2,5-di-*tert*-butyl-hydroquione from two type (b) C-O cleavage and 1,4-di-*tert*-butylbenzene from two type (a) C-O cleavage (a). The theoretical oxidation potentials for the two compounds are 3.55 V and 4.74 V, respectively. Degradation of the arms could also occur farther from the benzene ring. These potential products would have oxidation potentials close to that of 2,5-di-*tert*-butyl-1,4-dimethoxybenzene (~3.9 V).

We also considered the possibility that the observed experimental results were due to the second oxidation potential of the core 2,5-di-*tert*-butyl-1,4-dimethoxybenzene structure (lose 2 electrons per DDB unit). This turns out to be highly unlikely since the second oxidation potential is 10.53 V relative to the neutral species (5.25 V above the cation radical). We also considered including a $PF_6$ anion interacting with the cation radical in the calculation. In this case the second oxidation potential is still 5.16 V above the redox cation radical-$PF_6$ anion complex.

### 2.3.2. Mechanism for Release of the Redox Shuttle

A possible mechanism for release of a redox shuttle from the polymer matrix is shown in **Figure 12**. The first oxidation occurs on a DDB center followed by a C-O bond cleavage (type b, Figure 11; step I, Figure 12), which may be catalyzed by presence of the cathode surface. From computations it is thermodynamically favorable for one arm of this oxidized core to cleave (step I) so that it is replaced by a hydrogen on the benzene carbon as discussed in the next section. The oxidized DDB core may be in close proximity to a non-charged DDB as shown in Figure 12 (step II). The utilization of the polymer is ~74% when cycled at 4.1 to 3.0 V, thus there will be DDB cores remaining in the neutral form during the charging process. If there is an adjacent non-charged DDB core charge transfer can be realized from the charged DDB center with H atom terminated on one linker to this neighboring neutral DDB center (step III, Figure 12). The second oxidation occurs on the resulting neutral one-armed DDB species (step III, Figure 12). This occurs at a somewhat higher oxidation potential (step IV) than the first one due to the replacement of a more electron-donating alkoxyl group with a less electron-donating H atom. In the last step (V, Figure 12), another bond on ether linkage of the one armed DDB cleaves due to the second oxidation to release a charged DDB molecule into the solution that can act as a redox mediator shuttling between the cathode and anode.

This mechanism is consistent with the voltage profile observed for the overcharged cell. As shown in Figures 8 and 9, the second plateau in the first cycle is about 100 mV higher than that in the subsequent cycles. The ether-linkage cleavage occurring as a result of oxidation requires a higher voltage (4.3 V) than that of the soluble redox shuttles (4.2 V). In order for the second oxidation to happen, the positive charge on the redox core must be transferred to the polymer matrix or elsewhere, since placing two net positive charges on one DDB center is

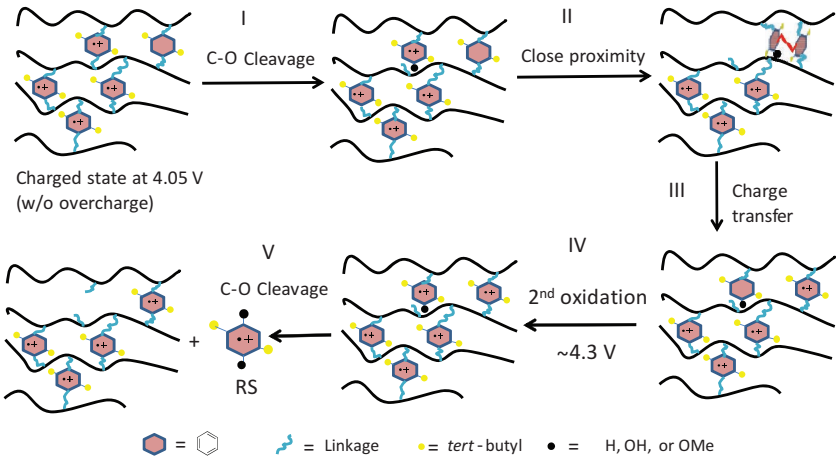


**Figure 12.** Proposed mechanism for the release of redox shuttle candidates.

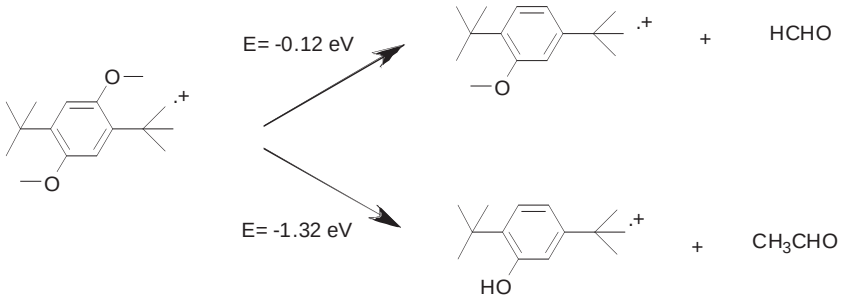


**Figure 13.** Possible decomposition reactions and their free energies.

highly unfavorable. One way that the charge can be transferred from the one-arm shuttle cation to the polymer matrix is by means of a nearby redox shuttle core in the polymer matrix that has a lower oxidation potential (Figure 12). Calculations on a *pi* stacking dimer composed of DDB and 2,5-di-*tert*-butyl-1-methoxybenzene show that for the cation radical the charge is mainly located on the DDB molecule due to its lower oxidation potential. Interestingly, a drop in potential can be observed during the second charging plateau in the first cycle. This might be caused by the switch from the decomposition reaction at 4.3 V to the redox shuttle activity at 4.2 V.

### *2.3.3. Reaction Energies for Model Systems*

In order to assess the possibility that oxidative cleavage of the DDB ether arms to form a redox shuttle as described above, we calculated various reaction energies for model systems. Some of the possible decomposition reactions of 2,5-di-*tert*-butyl-1,4-dimethoxybenzene cation radical are favorable. The question of which structure might leach out into the electrolyte will probably be controlled by kinetic factors and is beyond the scope of this study. As shown in **Figure 13**, two molecules with oxidation potentials close to 4.2 V had favorable reactions energies: the reaction of 2,5-di-*tert*-butyl-1,4-dimethoxybenzene cation radical to form 2,5-di-*tert*-butyl-1-methoxybenzene cation radical plus formaldehyde is favorable by 0.12 eV and the reaction of 2,5-di-*tert*-butyl-1,4-dimethoxybenzene cation radical to form 2,5-di-*tert*-butyl-1-hydroxybenzene cation radical plus acetaldehyde is favorable by 1.32 eV. Thus, the computational results provide evidence that an oxiditative cleavage of the DDB core structure could subsequently act as an efficient redox shuttle in the electrolyte for overcharge protection.

## 3. Conclusions

In conclusion, we have designed and synthesized a cross-linked polymeric material bearing the DDB redox center. This new polymeric cathode material shows good cycling performance with little charge/discharge voltage hysteresis. For the first time, we have demonstrated a dual function polymeric material that not only acts as a normal lithium battery cathode material, but also provides an intrinsic redox shuttle mechanism triggered by a high charge voltage. This new material can be blended with the lithium transition oxide cathode to provide not only additional capacity but also overcharge protection without introducing additional component in the electrolyte under normal operation conditions. Both experimental and computational studies provide evidence that an oxidized fragment from the polymer cathode at high potential dissolved into the electrolyte solution and subsequently acted as an efficient redox shuttle for overcharge protection.

## 4. Experimental Section

Unless otherwise noted, all reagents were purchased from Aldrich and used as received. $^{1}$H and $^{13}$C NMR experiments were performed on a Bruker model DMX 500 NMR spectrometer (11.7 T). FT-IR spectra were recorded on a Perkin-Elmer spectrum 100 instrument with an attenuated total reflection (ATR) sampling accessory.

For fabrication of the cathode, the prepared polymer **I** (20 wt%) was mixed with Super P conductive carbon black (60 wt%) and polyvinylidene fluoride (20 wt%) in N-methylpyrrolidone. The charge-discharge cycling performance was tested on a Maccor Electrochemical Analyzer in 2032-type coin cells using Li metal as a negative electrode, Celgard 2325 microporous film as the separator. The electrolyte was 1.2 M $LiPF_6$ dissolved in the mixture of EC/EMC (3:7). Cyclic voltammograms were obtained at a scan rate of 0.05 mV/s using a Solartron Analytical 1470E system.

*Synthesis of III*: 3-bromo-1-propanol (5g, 0.036 mol) was slowly added to a suspension of 2,5-di-*tert*-butylbenzene-1,4-diol (2.67 g, 0.012 mol) and cesium carbonate (10.9 g, 0.0336 mol) in 30 mL anhydrous dimethylformamide. After stirring at 70 °C for 16 h, the mixture was cooled down to room temperature and poured into ice water with stirring. The product was extracted with dichloromethane and washed with water. The organic solution was dried over anhydrous magnesium sulfate and the volatiles were evaporated under reduced pressure. The resulting residue was purified by column chromatography (silica, $CH_2Cl_2$: ethyl acetate = 10:1; $R_f$ = 0.25) to give **III** as white powder (1.4 g, 35%). $^{1}$H NMR (500 MHz, $CDCl_3$, $\delta$): 6. 85 (s, 2H), 4.10 (t, J = 6 Hz, 4H), 3.92 (t, J = 6 Hz, 4H), 2.09 (p, J = 6 Hz, 4H), 1.68 (br, 2H), 1.37 (s, 18H). $^{13}$C NMR (125 MHz, $CDCl_3$, $\delta$): 151. 1 (Ar-*C*), 136. 1(Ar-*C*), 112. 2 (Ar-*C*), 65. 9 (O-*C*$H_2$), 60. 6 (O-*C*$H_2$), 34. 6 (O-$CH_2CH_2CH_2$O-), 32. 6 (*C*$Me_3$), 29. 9 (C*Me*$_3$).

*Synthesis of II*: Triethylamine (620 µL, 4.46 mmol), 4-dimethylaminopyridine (40 mg) and compound **III** were added to a Schlenk flask charged with 30 mL of dry THF. The flask was immersed in ice bath and purged with Ar. Methacryloyl chloride (435 µL, 4.46 mmol) was added dropwise by syringe. After additional stirring for 2 h at 0 °C, the reaction mixture was allowed to attain room temperature and stirred for another 3 h. The mixture was quenched with distilled water. The product was extracted with dichloromethane and washed with distilled water. The organic solution was dried over anhydrous magnesium sulfate and the volatiles were evaporated under reduced pressure. The crude was purified by column chromatography (silica, hexane: ethyl acetate = 20:1) to give **II** as white powder (0.6 g, 68%). $^{1}$H NMR (500 MHz, $CDCl_3$, $\delta$): 6. 83 (s, 2H, Ar-H), 6.13 (br, 1H, = $CH_a$), 5.57 (m, 1H, = $CH_b$), 4.40 (t, J = 6 Hz, 4H), 4.08 (t, J = 6 Hz, 4H), 2.21 (p, J = 6 Hz, 4H), 1.96 (m, 6H), 1.37 (s, 18H). $^{13}$C NMR (125 MHz, $CDCl_3$, $\delta$): 167. 3 (O = *C*-O), 150. 9 (Ar-*C*), 136. 2 (acrylate = *C*), 136. 1 (acrylate = *C*), 125. 4 (Ar-*C*), 111. 9 (Ar-*C*), 64. 8 (O-*C*$H_2$), 61. 8 (O-*C*$H_2$), 34. 6 (O-$CH_2CH_2CH_2$O-), 29. 8 (*C*$Me_3$), 29. 1 (*C*$Me_3$), 18.3 (C = C-*Me*).

*Synthesis of Polymer I*: Azobisisobutyronitrile (AIBN) (6 mg) was added to the toluene solution of monomer **II** (0.6 g), The solution was degassed through three cycles of freeze-pump-thaw method. The mixture was stirred at 40 °C for 5 days. The viscous residue was quenched with methanol, and the white precipitate was filtered and dried under vacuum. The polymer is not soluble in common organic solvents.

*Computational Methods*: All calculations were done with Gaussian 03.[23] Molecules were optimized at the B3LYP/631G* level. Solvation effects were included at the B3LYP/631+G* level with the PCM solvation model and eps = 55.725 (with water as the default solvent) to mimic the carbonate electrolyte.[24] B3LYP/6311+G(3df,2p) single point calculations were also performed to assess for higher level basis set effects.

## Acknowledgements

This work was supported by the Center for Electrical Energy Storage: Tailored Interfaces, an Energy Frontier Research Center funded by the U.S. Department of Energy, Office of Science, Office of Basic Energy Sciences. Argonne National Laboratory is operated for the U.S. Department of Energy by UChicago Argonne, LLC, under contract DE-ACOZ-06CH11357.

Received: February 13, 2012
Revised: April 16, 2012
Published online: June 25, 2012

[1] M. Armand, J. M. Tarascon, *Nature* **2008**, *451*, 652.
[2] H. Chen, M. Armand, G. Demailly, F. Dolhem, P. Poizot, J. M. Tarascon, *ChemSusChem* **2008**, *4*, 348.
[3] P. Novák, K. Müller, K. S. V. Santhanam, O. Haas, *Chem. Rev.* **1997**, *97*, 207.
[4] H. Chen, M. Armand, M. Courty, M. Jiang, C. P. Grey, F. Dolhem, J. M. Tarascon, P. Poizot, *J. Am. Chem. Soc.* **2009**, *131*, 8984.
[5] J. Wang, J. Yang, J. Xie, N. Xu, *Adv. Mater.* **2002**, *14*, 963.
[6] H. Nishide, K. Koshika, K. Oyaizu, *Pure Appl. Chem.* **2009**, *81*, 1961.
[7] K. Oyaizu, H. Nishide, *Adv. Mater.* **2009**, *21*, 2339.
[8] K. Tamura, N. Akutagawa, M. Satoh, J. Wada, T. Masuda, *Macromol. Rapid Commun.* **2008**, *29*, 1944.
[9] K. S. Park, S. B. Schougaard, J. B. Goodenough, *Adv. Mater.* **2007**, *19*, 848.
[10] J. Zhang, L. Kong, L. Zhan, J. Tang, H. Zhan, Y. Zhou, C. Zhan, *Electrochem. Commun.* **2008**, *10*, 1551.
[11] Z. Song, H. Zhan, Y. Zhou, *Chem. Commun.* **2009**, 448.
[12] K. Liu, J. Zheng, G. Zhong, Y. Yang, *J. Mater. Chem.* **2011**, *21*, 4125.
[13] D. Häringer, P. Novák, O. Hass, B. Piro, M. C. Pham, *J. Electrochem. Soc.* **1999**, *146*, 2393.
[14] C. Buhrmester, J. Chen, L. Moshurchak, J. W. Jiang, R. L. Wang, J. R. Dahn, *J. Electrochem. Soc.* **2005**, *152*, A2390.
[15] J. Chen, C. Buhrmester, J. R. Dahn, *Electrochem. Solid-State Lett.* **2005**, *8*, A59.
[16] J. R. Dahn, J. W. Jiang, L. M. Moshurchak, M. D. Fleischauer, C. Buhrmester, L. J. Krause, *J. Electrochem. Soc.* **2005**, *152*, A1283.
[17] L. Zhang, Z. Zhang, H. Wu, K. Amine, *Energy Environ. Sci.* **2011**, *4*, 2858.
[18] W. Weng, Z. Zhang, P. C. Redfern, L. A. Curtiss, K. Amine, *J. Power Sources* **2011**, *196*, 1530.
[19] P. Nesvadba, L. B. Folger, P. Maire, P. Novák, *Synt. Met.* **2011**, *161*, 259.
[20] B. Dizman, L. J. Mathias, *J. Polym. Sci., Part A: Polym. Chem.* **2005**, *43*, 5844.
[21] L. M. Moshurchak, C. Buhrmester, R. L. Wang, J. R. Dahn, *Electrochim. Acta* **2007**, *52*, 3779.
[22] L. M. Moshuchak, M. Bulinski, W. M. Lamanna, R. L. Wang, J. R. Dahn, *Electrochem. Commun.* **2007**, *9*, 1497.
[23] Gaussian 03, Revision C.02, M. J. Frisch, G. W. Trucks, H. B. Schlegel, G. E. Scuseria, M. A. Robb, J. R. Cheeseman, J. A. Montgomery Jr., T. Vreven, K. N. Kudin, J. C. Burant, J. M. Millam, S. S. Iyengar, J. Tomasi, V. Barone, B. Mennucci, M. Cossi, G. Scalmani, N. Rega, G. A. Petersson, H. Nakatsuji, M. Hada, M. Ehara, K. Toyota, R. Fukuda, J. Hasegawa, M. Ishida, T. Nakajima, Y. Honda, O. Kitao, H. Nakai, M. Klene, X. Li, J. E. Knox, H. P. Hratchian, J. B. Cross, C. Adamo, J. Jaramillo, R. Gomperts, R. E. Stratmann, O. Yazyev, A. J. Austin, R. Cammi, C. Pomelli, J. W. Ochterski, P. Y. Ayala, K. Morokuma, G. A. Voth, P. Salvador, J. J. Dannenberg, V. G. Zakrzewski, S. Dapprich, A. D. Daniels, M. C. Strain, O. Farkas, D. K. Malick, A. D. Rabuck, K. Raghavachari, J. B. Foresman, J. V. Ortiz, Q. Cui, A. G. Baboul, S. Clifford, J. Cioslowski, B. B. Stefanov, G. Liu, A. Liashenko, P. Piskorz, I. Komaromi, R. L. Martin, D. J. Fox, T. Keith, M. A. Al-Laham, C. Y. Peng, A. Nanayakkara, M. Challacombe, P. M. W. Gill, B. Johnson, W. Chen, M. W. Wong, C. Gonzalez, J. A. Pople, Gaussian, Inc., Wallingford CT, **2004**.
[24] J. M. Vollmer, L. A. Curtiss, D. R. Vissers, K. Amine, *J. Electrochem. Soc.* **2004**, *151*, A178.